

Longitudinal Magnetoacoustic Absorption*

CARLO JACOBONI

Istituto di Fisica della Università di Modena, Modena, Italy

AND

E. W. PROHOFKY

Department of Physics, Purdue University, Lafayette, Indiana 47907

(Received 12 May 1970)

The effect of a longitudinal magnetic field in electroacoustic absorption is studied in this paper in the extreme quantum limit, when only the lowest Landau level of the electrons is occupied. The magnetic field enters the theory through its effect on the electronic relaxation time. The case of relaxation times as given by acoustic-phonon scattering has been fully solved analytically, while for ionized-impurity scattering, numerical integrations are necessary. Numerical examples are shown and discussed.

I. INTRODUCTION

Experimental results¹⁻³ show that the absorption coefficient α of an acoustic wave in semiconductors is affected by the presence of a magnetic field applied to the sample parallel to the direction of propagation of the acoustic wave. In these semiconductors the fields generated by the acoustic wave which contribute appreciably to its absorption by charge carriers are the piezoelectric field and the deformation-potential field.⁴ The latter is always parallel to the acoustic wave vector, and so is the piezoelectric field when it is not negligible. Therefore, a simple theory which takes into account the magnetic field only through its effect on the orbits of the carriers gives no explanation of the longitudinal magnetic-field dependence of the absorption coefficient.⁵

Good agreement with the experimental results of Ref. 1 was obtained by the authors⁶ by taking into account the effect of the magnetic field on the electronic relaxation time τ . The change in τ is caused in this theory by the Landau quantization of the electronic orbits. This interpretation has been confirmed by recent results of Bray's group.³ They observed resonant acoustoelectric gain when the energy difference between two Landau levels is equal to the energy of optical phonons in the semiconductor. At these field intensities there is a drastic decrease in τ ; the absorption coefficient (or amplification coefficient, when a high electric field is applied) varies inversely with τ at these frequencies, so that maxima in α occur.

In the letter mentioned above⁶ the authors gave only the results of the theory for the particular case when the carrier relaxation time is essentially determined by ionized impurity scattering, as was probably the case in the experiments discussed.

In this paper we present the theory of this effect in greater detail and extend it to the case where the electronic relaxation time is dominated by the scattering from acoustic phonons. We again confine ourselves, as in Ref. 6, to the extreme quantum limit, when the magnetic field is so high that the spacing $\hbar\omega_c$ between

the Landau levels is much larger than the thermal energy kT ; all the conduction electrons are therefore in the lowest quantum state.

In the present calculations the transport coefficients are obtained by means of Chambers' method, which is equivalent to solving the Boltzmann transport equation. This classical equation may not be valid in the region of high magnetic fields considered here. In our case, however, the Boltzmann equation is used only for the distribution of the components of the electron velocities parallel to the magnetic field and to the wave vector, where the acoustically induced forces act, and the magnetic field is not effective. In the plane perpendicular to the magnetic field no effective forces are induced by the acoustic wave. All the electrons may be assumed to occupy, in a stationary distribution, the eigenstates of the Hamiltonian belonging to the different Landau levels. (In particular, in our case all the electrons lie in the lowest Landau level.) Therefore, the use of the Boltzmann transport equation is justifiable, as regards the Landau quantization, for the case of longitudinal magnetic fields.^{7,8}

A different problem which arises in using the classical transport equation is related to the quantum interference effects between the electron waves and the acoustic wave. This fact makes our calculations invalid at very high ultrasonic frequencies. In InSb, for example, the quantum "electron recoil"¹ becomes significant at frequencies around 10^{10} – 10^{11} rad/sec, while for substances with higher electronic effective masses the classical theory validity limit is higher. However, we extend the range of frequencies considered in this paper well above this limit and even above the limit of frequencies existing in solids in order to give a complete, consistent picture of the classical theory in both low- and high-frequency limits.

The theory is given in Sec. II, while numerical examples are shown and discussed in Sec. III.

II. THEORY

Following the lines of the well-known paper by Cohen, Harrison, and Harrison,⁹ we assume that an

acoustic wave with velocity field

$$\mathbf{u}(\mathbf{r}, t) = \mathbf{u}_0 \exp[i(\mathbf{q}\mathbf{r} - \omega t)] \quad (1)$$

propagates in a continuous elastic medium with background charge density $n_0 e$ and n_0 carriers per unit volume with charge $-e$ and scalar effective mass m . These carriers are assumed to obey classical statistics. The elastic medium interacts with the carriers through a deformation potential and a piezoelectric field. Pure electromagnetic interaction of the carriers with the background charge and currents can be neglected in semiconductors, due to the low charge density. We neglect also the collision drag effect,¹⁰ since it is negligible with respect to deformation potential and piezoelectric interactions.

A magnetic field \mathbf{H} is applied parallel to the wave vector $\mathbf{q} \parallel z$. It is assumed to be so high that only the lowest Landau level is available to the electrons at the temperature T of the sample. The carrier distribution function in the equilibrium condition is then a function of the z component v_z of the velocity of the carriers alone:

$$f_0^H(v_z) = [n_0 / (\sqrt{\pi} v_0)] \exp[-(v_z/v_0)^2], \quad (2)$$

where v_0 is the thermal velocity $(2kT/m)^{1/2}$.

The theory of the electronic contribution to the acoustic absorption proceeds now as for the case without magnetic field¹¹ because the effective force acting on the carriers is parallel to the wave-propagation direction and, therefore, to the longitudinal magnetic field. The result is the familiar expression for the absorption coefficient in the linear approximation:

$$\alpha = (\omega^2 A^2 / \rho v_s^3 \sigma_0) \operatorname{Re}[(\sigma' / \sigma_0) - i(\omega / \omega_r)]^{-1}, \quad (3)$$

where

$$A^2 = e^2 + (\kappa q C / 4\pi e)^2, \quad (4)$$

ρ is the density of the crystal, v_s is the velocity of the

sound wave, σ_0 is the dc conductivity of the sample,¹² ω_r is the dielectric relaxation frequency $4\pi\sigma_0/\kappa$, κ is the dielectric constant, e and C are the piezoelectric and the deformation-potential constants, defined in such a way that the piezoelectric polarization, parallel to \mathbf{q} by assumption, is given by

$$P = -(u/v_s)e, \quad (5)$$

and the deformation-potential tensor \mathbf{C} gives

$$\mathbf{q} \cdot \mathbf{C} \cdot \mathbf{u} = qCu. \quad (6)$$

σ' represents the conductivity as modified by the diffusion:

$$\sigma' = \sigma / (1 - R). \quad (7)$$

The transport coefficients σ and R are now evaluated over the one-dimensional distribution function. They have the form¹¹

$$\sigma = \frac{ie^2}{kTq} \int_{-\infty}^{+\infty} \frac{v_z^2 f_0^H dv_z}{v_s + i/(q\tau) - v_z}, \quad (8)$$

$$R = \frac{i}{n_0} \int_{-\infty}^{+\infty} \frac{v_z f_0^H dv_z}{\omega\tau[v_s + i/(q\tau) - v_z]}. \quad (9)$$

Here the relaxation time τ of the electrons is a function of both the electronic energy (or v_z) and the magnetic field. The expressions for τ used in Ref. 11 must now be substituted by the equivalent expressions valid when the magnetic field is applied.

In what follows we shall discuss two cases of practical importance. First we give a complete analytical solution to the case of τ as given by acoustic phonon scattering; then we discuss the case of τ as given by ionized impurity scattering, but in this case, due to the complexity of the formulas, numerical integrations are necessary for the transport coefficients.

Acoustic Phonon Scattering

When the relaxation time of the carriers is essentially due to the scattering from acoustic phonons, at the extreme quantum limit Argyres and Adams⁷ give

$$\tau = \tau_H^A(v_z) = (2\tau_a kT / \hbar\omega_c) (|v_z| / v_0), \quad (10)$$

where τ_a is a constant with the dimension of time such that the relaxation time of the electrons due to the same type of scattering in absence of the magnetic field is given by $\tau_a v_0 / v$. When this expression for τ is substituted into Eq. (8), the transport coefficient σ becomes, after simple calculations,

$$\frac{\sigma_H^A(\omega)}{\sigma_0} = \frac{2i}{(\sqrt{\pi})ql_0} \left(\int_0^\infty \frac{\xi^3 \exp(-\xi^2) d\xi}{\xi^2 + \xi s + iP} - \int_0^\infty \frac{\xi^3 \exp(-\xi^2) d\xi}{\xi^2 - \xi s - iP} \right), \quad (11)$$

where $P = \hbar\omega_c / (2kTql_a)$, $l_a = v_0\tau_a$, $l_0 = v_0\tau_0$, $s = v_s/v_0$, and τ_0 is defined in such a way that $\sigma_0 = n_0 e^2 \tau_0 / m$. We note that τ_0 and τ_a are related by the equation $\tau_a = \frac{3}{4}(\sqrt{\pi})\tau_0$. We may simplify the integrands in Eq. (11) by carrying out the division. We then obtain

$$\frac{\sigma_H^A(\omega)}{\sigma_0} = -\frac{2is}{ql_0} + \frac{2i}{(\sqrt{\pi})ql_0} \left(\int_0^\infty \frac{(s^2 - iP)\xi + isP}{\xi^2 + s\xi + iP} \exp(-\xi^2) d\xi - \int_0^\infty \frac{(s^2 + iP)\xi + isP}{\xi^2 - s\xi - iP} \exp(-\xi^2) d\xi \right). \quad (12)$$

We can again transform the ratios in the integrands into simpler ratios:

$$\frac{\sigma_H^A(\omega)}{\sigma_0} = -\frac{2is}{ql_0} + \frac{is^2}{(\sqrt{\pi})ql_0} \left[\left(1 - iM + \frac{3iM-1}{(1-4iM)^{1/2}}\right) \int_0^\infty \frac{\exp(-\xi^2)d\xi}{\xi + iz_-} + \left(1 - iM - \frac{3iM-1}{(1-4iM)^{1/2}}\right) \int_0^\infty \frac{\exp(-\xi^2)d\xi}{\xi - iz_+} \right. \\ \left. - \left(1 + iM - \frac{3iM+1}{(1+4iM)^{1/2}}\right) \int_0^\infty \frac{\exp(-\xi^2)d\xi}{\xi + iz_-^*} - \left(1 + iM + \frac{3iM+1}{(1+4iM)^{1/2}}\right) \int_0^\infty \frac{\exp(-\xi^2)d\xi}{\xi - iz_+^*} \right], \quad (13)$$

where

$$z_{\pm} = \frac{1}{2}is[(1-4iM)^{1/2} \pm 1], \quad (14)$$

$M = P/s^2$, and the asterisk indicates complex conjugation. Now the integrals can be expressed in terms of the exponential integral function E_1 and the function w related to the error function, since¹³

$$\int_0^\infty \frac{\exp(-t^2)dt}{t+C} = \frac{1}{2} \exp(-C^2) E_1(-C^2) \mp \frac{1}{2}i\pi w(\pm C),$$

where the upper (lower) signs hold if the imaginary part of C is larger (less) than zero. We then obtain

$$\frac{\sigma_H^A(\omega)}{\sigma_0} = -\frac{2is}{ql_0} + \frac{is^2}{(2\sqrt{\pi})ql_0} \left\{ \left(1 - iM + \frac{3iM-1}{(1-4iM)^{1/2}}\right) [\exp(z_-^2) E_1(z_-^2) - i\pi w(iz_-)] \right. \\ + \left(1 - iM - \frac{3iM-1}{(1-4iM)^{1/2}}\right) [\exp(z_+^2) E_1(z_+^2) + i\pi w(iz_+)] \\ - \left(1 + iM - \frac{3iM+1}{(1+4iM)^{1/2}}\right) [\exp(z_-^{2*}) E_1(z_-^{2*}) - i\pi w(iz_-^*)] \\ \left. - \left(1 + iM + \frac{3iM+1}{(1+4iM)^{1/2}}\right) [\exp(z_+^{2*}) E_1(z_+^{2*}) + i\pi w(iz_+^*)] \right\}. \quad (15)$$

Now we note that $w(z^*) = w^*(-z)$ and $E_1(z^*) = E_1^*(z)$, and we obtain

$$\operatorname{Re} \left(\frac{\sigma_H^A(\omega)}{\sigma_0} \right) = \frac{s^2}{(\sqrt{\pi})ql_0} \operatorname{Re} \left\{ (M+i) [\exp(z_+^2) E_1(z_+^2) + \exp(z_-^2) E_1(z_-^2)] \right. \\ \left. + \frac{3M+i}{(1-4iM)^{1/2}} [\exp(z_+^2) E_1(z_+^2) - \exp(z_-^2) E_1(z_-^2)] \right\}, \quad (16)$$

$$\operatorname{Im} \left(\frac{\sigma_H^A(\omega)}{\sigma_0} \right) = -\frac{2s}{ql_0} + \frac{(\sqrt{\pi})s^2}{ql_0} \operatorname{Re} \left\{ (M+i) [w(iz_+) - w(iz_-)] + \frac{3M+i}{(1-4iM)^{1/2}} [w(iz_+) + w(iz_-)] \right\}. \quad (17)$$

Substitution of τ as given in Eq. (10) into Eq. (9) leads to the expression for $R_H^A(\omega)$. We follow the same lines as for $\sigma_H^A(\omega)$, and the result is

$$\operatorname{Re}[R_H^A(\omega)] = \frac{1}{2}(\pi)Ms \operatorname{Re}\{[w(iz_+) - w(iz_-)] + (1-4iM)^{-1/2}[w(iz_+) + w(iz_-)]\}, \quad (18)$$

$$\operatorname{Im}[R_H^A(\omega)] = -(Ms/2\sqrt{\pi}) \operatorname{Re}\{[\exp(z_+^2) E_1(z_+^2) + \exp(z_-^2) E_1(z_-^2)] \\ + (1-4iM)^{-1/2}[\exp(z_+^2) E_1(z_+^2) - \exp(z_-^2) E_1(z_-^2)]\}. \quad (19)$$

Ionized Impurity Scattering

When the relaxation time of the carriers is essentially due to the scattering with ionized impurities, at the extreme quantum limit, the expression for τ given by Argyres and Adams⁷ has the form

$$\tau = \tau_H^I(v_z) = \tau_i \left| \frac{v_z}{v_0} \right|^3 \frac{1 + \frac{1}{4}(v_0/v_z)^2(\epsilon_s/kT)}{I(\gamma)}, \quad (20)$$

where

$$I(\gamma) = \int_0^\infty x e^{-x} \frac{dx}{x+\gamma} = 1 - \gamma e^\gamma E_1(\gamma), \quad (21)$$

$$\gamma = (\epsilon_s/\hbar\omega_c) [1 + 4(v_z/v_0)^2(kT/\epsilon_s)], \quad (22)$$

$$\epsilon_s = \hbar^2/2mr_s^2, \quad (23)$$

$$r_s^2 = \kappa kT/4\pi e^2 n_0, \quad (24)$$

and τ_i is a constant with the dimension of time such that

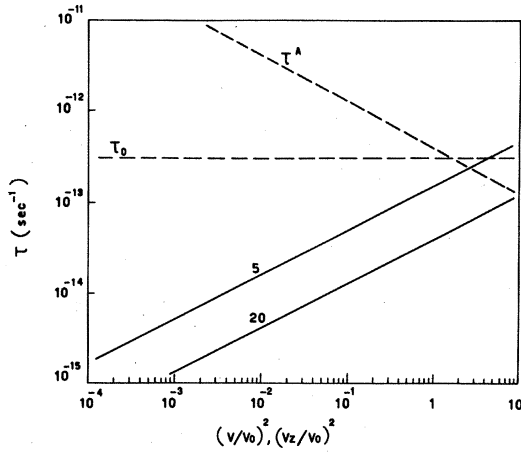


FIG. 1. Relaxation times for GaAs at 77°K. The horizontal dashed line gives the constant τ_0 . The dashed line labelled by τ^4 gives the relaxation time due to acoustic phonon scattering in absence of magnetic field. Solid lines give τ_H^4 , as given by Eq. (10), due to acoustic phonon scattering with applied magnetic field. The numbers on the solid lines indicate the values of the magnetic field as specified in the text. The independent variable in the x axis is $(v/v_0)^2$ for the dashed lines and $(v_z/v_0)^2$ for the solid lines.

the relaxation time of the electrons due to the same type of scattering in absence of magnetic field is given by the Brooks-Herring formula

$$\tau_z(v/v_0)^3 [\ln(1+\beta) - \beta/(1+\beta)]^{-1}, \quad (25)$$

$$\beta = 4(v/v_0)^2 (kT/\epsilon_s). \quad (26)$$

Comparing the expressions in Eqs. (20)–(24) due to ionized impurity scattering with the previous expression in Eq. (10) for the acoustic phonon case, and taking into account the form of the final results of the previous case, the reader may well imagine that we were not able to give an analytical solution for the

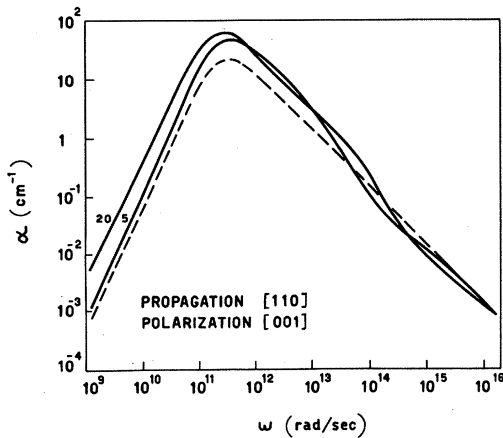


FIG. 2. Absorption coefficient as function of frequency for GaAs at 77°K. The dashed line refers to $H=0$. Solid lines refer to the same values of the magnetic field as in Fig. 1. (See Ref. 14.)

transport coefficients in the case of impurity scattering. We simply note that σ and R may be given the following forms:

$$\frac{\sigma}{\sigma_0} = \frac{2i}{(\sqrt{\pi})\omega\tau_0} \int_0^\infty \frac{(\sqrt{x})e^{-x}[1+i/\omega\tau]}{[1+i/\omega\tau]^2 - x/s^2} dx, \quad (27)$$

$$R = \frac{i}{(\sqrt{\pi})s^2} \int_0^\infty \frac{(\sqrt{x})e^{-x}(1/\omega\tau)}{[1+i/\omega\tau]^2 - x/s^2} dx. \quad (28)$$

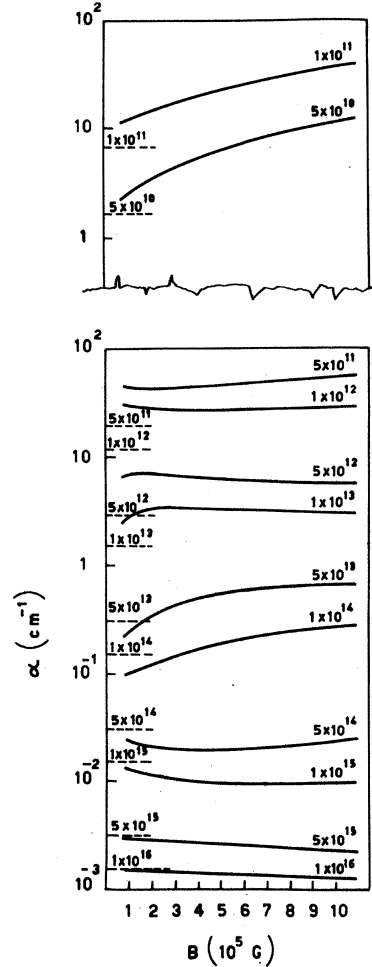


FIG. 3. Absorption coefficient as function of magnetic field for GaAs at 77°K, for several values of the frequency. The dashed lines indicate the values of α for $H=0$. The numbers on the curves are the corresponding values of ω . (See Ref. 14.)

These expressions have been used for the numerical calculations in the following section for the case of impurity scattering. They have also been used for the acoustic phonon case to check the analytical solution in Eqs. (16)–(19).

III. NUMERICAL RESULTS AND DISCUSSION

Two numerical examples will be developed and discussed in this section. In the first example we consider

n-type GaAs at 77°K with an acoustic wave propagating along a [110] direction with polarization in the [001] direction as in the numerical example in Ref. 11. The set of parameters used are

$$\begin{aligned}\sigma_0 &= 2.0 \times 10^{13} \text{ sec}^{-1}, & n_0 &= 1.7 \times 10^{16} \text{ cm}^{-3}, \\ v_s &= 3.35 \times 10^5 \text{ cm/sec}, & \kappa &= 12.5, \\ \epsilon_{14} &= 6.8 \times 10^4 \text{ esu/cm}^2, & m &= 0.067 m_0, \\ \rho &= 5.35 \text{ g/cm}^3,\end{aligned}$$

m_0 being the mass of free electrons, and ϵ_{14} the piezoelectric constant. No deformation potential is present ($C=0$) since the acoustic wave has transverse polarization. For this particular geometry ϵ is simply ϵ_{14} . In this first numerical example we consider acoustic phonon scattering dominant in the determination of the carrier relaxation time.

In Fig. 1 the relaxation time is shown as a function of the energy. More precisely, the independent variable on the x axis is $(v/v_0)^2$ for the dashed lines representing $\tau_0 = \text{const}$ and τ^I as given by acoustic phonon scattering in absence of the magnetic field. Both curves for zero magnetic field are normalized to the same conductivity σ_0 ; no other parameters are necessary for the curves with $H \neq 0$. For the solid lines, representing $\tau_H^A(v_z)$, the independent variable on the x axis is $(v_z/v_0)^2$. The numbers on the solid lines refer to two different values of the magnetic field: The number 5 labels the curve for $H = 1.91 \times 10^5$ G ($\hbar\omega_c/kT = 5$); the number 20 labels the curve for $H = 7.64 \times 10^5$ G ($\hbar\omega_c/kT = 20$).

In Fig. 2 the absorption coefficient for this first numerical example is shown as a function of frequency.¹⁴ The dashed line refers to the case with no magnetic field,¹¹ while solid lines refer to the same values of the magnetic field as in Fig. 1. At low frequencies, where $ql \ll 1$ and the local Hutson and White theory holds, α is proportional to σ^{-1} . Since the relaxation time of the electrons in the presence of the magnetic field is smaller than for $H=0$ for all effective values of the energy (see Fig. 1), we have a decrease of σ and an increase of α with the applied magnetic field. Furthermore, τ_H^A and, therefore, σ are proportional to H^{-1} so that α is proportional to H . Finally, the reduction of τ due to the magnetic field has the consequence of expanding the range of validity of the local theory toward higher frequencies.

In the intermediate frequency region of $ql \gtrsim 1$ the local nature of the conductivity breaks down as the carriers travel through many wavelengths. This smears out the ability to bunch the carriers in phase with the acoustic wave due to the difference in velocity between carriers and wave. This has been called the ql effect in a previous publication.¹¹ The magnetic field, by reducing τ , reduces the ql effect, and we have larger α in the intermediate frequency region as well.

At still higher frequencies the discussion of attenu-

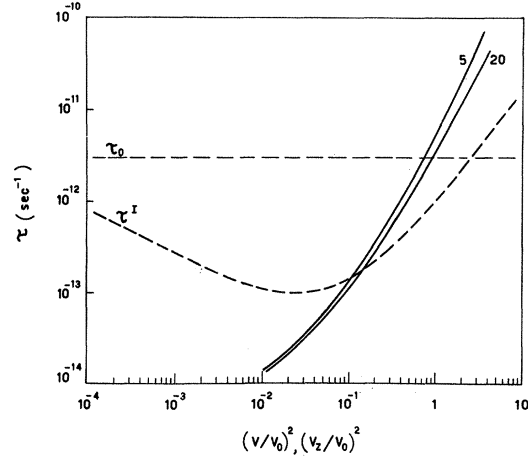


FIG. 4. Relaxation times for InSb at 20°K. The horizontal dashed line gives the constant τ_0 . The dashed line labeled by τ^I gives the relaxation time as due to ionized impurity scattering in absence of magnetic field. Solid lines give τ_H^I , as given by Eq. (20), due to ionized impurity scattering with applied magnetic field. The numbers on the solid lines indicate the values of the magnetic field as specified in the text. The independent variables in the x axis are the same as in Fig. 1.

ation in terms of simple magnetoresistance effects in σ breaks down. For $ql \gg 1$ individual electrons which become synchronized with the wave motion (i.e., resonant interaction) dominate the attenuation. Only very slow electrons can remain synchronous and so the dominant electrons shift to lower energy as the frequency increases. These electrons with lowest energy are those which have their lifetime reduced most by the magnetic field. This reduction in lifetime reduces the synchronous time, the electron wave interaction is ultimately reduced, and the attenuation decreases. This explains the inversion of the curves in the right-hand part of Fig. 2. It must be noted, however, that the right-hand part of Fig. 2 refers to values of the frequency which are outside the range of validity of our classical theory.¹⁴

In Fig. 3 we show the absorption coefficient as a function of the magnetic field for several values of the frequency.¹⁴ To understand the main features of this figure we should remember that τ_H^A decreases with increasing magnetic fields as H^{-1} [see Eq. (10)]. Furthermore, the absorption coefficient α depends upon τ essentially through the product $\omega\tau$ (or ql) so that a sort of displacement law holds according to which similar behavior of α can be obtained by increasing the frequency or by increasing τ (i.e., decreasing the magnetic field). Now, at low values of ω , or high values of the magnetic field, when $\langle ql \rangle \ll 1$ and the local theory holds, α increases with H as we have seen above. This can be seen in the two upper curves ($\omega = 1 \times 10^{11}$ and 5×10^{10} rad/sec) and in the right-hand part of the curves for $\omega = 5 \times 10^{11}$ and 1×10^{12} rad/sec. At higher values of ω , or lower values of H , when ql becomes comparable with unity, the decrease in τ due to the increase of H is

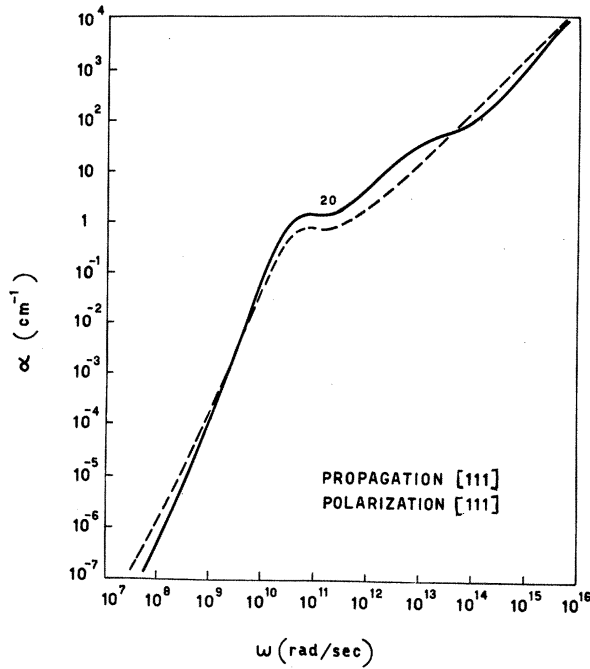


FIG. 5. Absorption coefficient as function of frequency for InSb at 20°K. The dashed line refers to $H=0$. The solid line refers to $H=38.5$ kG ($\hbar\omega_c/kT=20$). (See Ref. 14.)

more effective in reducing the ql effect than in reducing σ , so that σ increases and α decreases with the magnetic field. This explains the left-hand part of the 5×10^{11} and 1×10^{12} curves and the right-hand part of the next two curves. If $\omega\tau$ is further increased, the diffusion becomes dominant, lower τ reduces the diffusion and therefore increases α so that α increases with the magnetic field, as can be seen in the left-hand part of the 5×10^{12} and 1×10^{13} curves, in the next two curves, and in the right-hand part of the 5×10^{14} and 1×10^{15} curves. For values of the frequency so high that the diffusion already washes out any bunching, τ controls the resonance of the electrons travelling with the wave: Lower τ corresponds to poorer resonance so that α decreases with increasing H , as can be seen in the last curves of Fig. 3. Finally, for still higher values of $\omega\tau$ we reach the high-frequency limit and no distinction exists for $H=0$ or $H \neq 0$ (this limit is independent of τ), as can be seen in the left-hand part of the last two curves in Fig. 3.

In the second numerical example we consider a longitudinal wave propagating along a $[111]$ direction in InSb at 20°K. The set of parameters used is

$$\begin{aligned} n_0 &= 1.0 \times 10^{13} \text{ sec}^{-1}, & n_0 &= 1.75 \times 10^{14} \text{ cm}^{-3}, \\ v_s &= 3.94 \times 10^5 \text{ cm/sec}, & \kappa &= 18, \\ e_{14} &= 1.8 \times 10^4 \text{ esu/cm}^2, & m &= 0.013 m_0, \\ \rho &= 5.78 \text{ g/cm}^3, & C &= 1.32 \times 10^{-11} \text{ ergs.} \end{aligned}$$

For this particular geometry e is given by $(2/\sqrt{3})e_{14}$,

and we have deformation-potential coupling in addition to piezoelectric coupling. This second numerical example will be considered as one in which ionized impurity scattering is dominant in the determination of the carrier relaxation time. This example corresponds to the physical situation of Nill and McWhorter's experiments.¹ A comparison with the experimental results is given in Ref. 6. The agreement between theoretical and experimental results should improve by taking into account quantum electron recoil in the interaction between electrons and the acoustic wave.¹

In Fig. 4 the relaxation time is shown as a function of the energy. The independent variables along the x axis are the same as in Fig. 1. The numbers on the solid lines refer to $H=9.63$ kG and 38.5 kG corresponding to the same values of the parameter $\hbar\omega_c/kT$ as in the first example. Both curves for zero magnetic field are again normalized to the same value of σ_0 , and no other parameters are necessary for the curves for $H \neq 0$. We note that τ_H^I is very slightly dependent on the particular value of the magnetic field. This determines a slight dependence of α itself upon the particular value of H , so that we do not give the equivalent of Fig. 3 for this second example.

In Fig. 5 the absorption coefficient is shown as a function of frequency¹⁴ for the case of no magnetic field¹¹ and of $H=38.5$ kG ($\hbar\omega_c/kT=20$). Since the electronic relaxation time τ_H^I in presence of the magnetic field is higher than for $H=0$ in the range of energies which are important in dc conditions, we have negative dc magnetoresistance. Therefore, at low frequencies, where the local theory holds, α_H^I is smaller than in the case of no magnetic field. For the same reason, however, we reach the condition $ql \approx 1$, where the ql effect becomes effective, at lower frequencies when $H \neq 0$ than when $H=0$. Since the ql effect tends to increase the absorption coefficient, we have the crossing of the two curves shown in Fig. 5 at $\omega \approx 2 \times 10^9$ rad/sec. For higher values of the frequency the behavior of the curves in Fig. 5 is the same as in Fig. 2 (except for the ω^2 dependence of the deformation potential coupling), due to the similar dependence of τ_H^I and τ_H^A upon energy. This can be seen in Figs. 1 and 4. As we mentioned above, however, in this second case we have very little dependence of the absorption coefficient upon the magnetic field.

To conclude: In this paper we have studied the effect of a strong longitudinal magnetic field on the electronic contribution to the acoustic absorption in semiconductors. We considered only the extreme quantum limit, when only the lowest Landau level is available to the electrons. In our theory the effect of the magnetic field on the absorption coefficient is entirely due to the effect of the magnetic field on the electronic relaxation time.

Two cases have been considered and discussed: (i) For τ as given by acoustic phonon scattering, a complete analytical solution is given to the transport prob-

lem. The absorption in the presence of the magnetic field is in general higher than for $H=0$ and it is a function of H . (ii) For τ as given by ionized impurity scattering, the integrals of the transport coefficients are too complicated to be evaluated analytically. The absorption coefficient in the presence of the magnetic field, with respect to its value without magnetic field,

is lower at low frequencies and higher at high frequencies.

In both cases the absorption coefficient in the presence of the magnetic field becomes smaller than for $H=0$ before reaching the high-frequency limit, but these frequencies are beyond those of interest in ultrasonics.

* Partially supported by Advanced Research Projects Agency of the Department of Defense.

¹ K. W. Nill and A. L. McWhorter, J. Phys. Soc. Japan Suppl. **21**, 755 (1966).

² C. Hamaguchi, J. B. Ross, and R. Bray, Bull. Am. Phys. Soc. **14**, 353 (1969).

³ V. Dolat and R. Bray, Phys. Rev. Letters **24**, 262 (1970).

⁴ H. N. Spector, Solid State Phys. **19**, 291 (1967).

⁵ C. Jacoboni and E. W. Prohofsky, J. Appl. Phys. **40**, 454 (1969).

⁶ C. Jacoboni and E. W. Prohofsky, Phys. Letters **A28**, 765 (1969).

⁷ P. N. Argyres and E. N. Adams, Phys. Rev. **104**, 900 (1956).

⁸ L. M. Roth and P. N. Argyres, Semicond. Semimet. **1**, 159 (1966).

⁹ M. H. Cohen, M. J. Harrison, and W. A. Harrison, Phys. Rev. **117**, 937 (1960).

¹⁰ T. Holstein, Phys. Rev. **113**, 479 (1959).

¹¹ C. Jacoboni and E. W. Prohofsky, Phys. Rev. B **1**, 697 (1970).

¹² σ_0 is the dc conductivity of the sample in absence of the magnetic field. Its presence here is simply due to σ_0 and ω_c put in the expression inside the brackets in Eq. (3) to make it non-dimensional.

¹³ *Handbook of Mathematical Functions*, edited by M. Abramowitz and I. A. Stegun (National Bureau of Standards, Washington, D.C., 1964).

¹⁴ In order to give a full picture of the present classical theory, also in the high-frequency limit, the curves are plotted up to frequencies higher than those existing in solids.

Field-Dependent Photoinjection Efficiency of Carriers in Amorphous Se Films

H. SEKI

IBM Research Laboratory, San Jose, California 95114

(Received 10 July 1970)

A concept of a field-dependent photoinjection process has been developed and applied to the low-energy light data from photodischarge measurements reported by Pai and Ing, and by Tabak and Warter. The model involves a field-dependent photogeneration of free carriers based on a Poole-Frenkel-type effect. Comparison with data tends to support the idea that the intermediate states are excitons. It is shown that the derived expression for the photoinjection efficiency fits the available experimental data on holes rather well for the entire range of field at room temperature. Indications are that the expression is valid down to about 250°K. The low-field data is shown to be highly dependent upon the mobility and the recombination velocity. Based on the reported experimental data, the recombination velocity and the effective band gap are found to be 200 cm/sec and 2.65 eV, respectively.

INTRODUCTION

In recent papers Pai and Ing,¹ and Tabak and Warter² have reported some measurements indicating a field-dependent photogeneration of free carriers in the photodecay process of amorphous Se. In both cases they attempted to explain their results in terms of the Poole-Frenkel³ effect, but could not account for their data quantitatively over the entire range of field. In this paper it is shown that by a modified interpretation which introduces the concept of a photoinjection efficiency, their results for low light energies can indeed be explained in terms of the Poole-Frenkel effect.

In the second section, the concept of photoinjection efficiency is developed, and in the third section the Poole-Frenkel effect is introduced into the generation efficiency for low-energy light. Comparison with the

reported experimental data is presented in the fourth section.

FREE-CARRIER GENERATION RATE VERSUS INJECTION RATE

The essential point of this paper is to make a distinction between the free-carrier photogeneration rate and the free-carrier photoinjection rate. In view of this distinction, the data reported by Pai and Ing,¹ and Tabak and Warter² directly represents the latter rather than the former. It was pointed out by Many⁴ that even if the free-carrier generation efficiency is unity, the injection current is dependent on the field, recombination velocity, and the mobility. Here the concept of a field-dependent generation rate has been added. It should be mentioned that Pai and Ing¹ attributed the low-field behavior of their data to